Australian Journal of Basic and Applied Sciences, 4(8): 3770-3779, 2010
ISSN 1991-8178

Development of the Propagation Paths and Deriving Observer of Feedforward Active Noise Control System by Using State-Space Formulation

Mazin T. Muhssin, R.K. Raja Ahmad, Mohammad H. Marhaban, Payam Shafiei Bafti

Department of Electrical & Electronic Engineering, Faculty of Engineering, University Putra Malaysia Selangor Darul Ehsan, Malaysia.

Abstract: This paper presents the derivation and simulation of the propagation paths of a feedforward active noise control (ANC) system in one dimensional free-field medium using state-space model (SSM) instead of Finite Impulse Response (FIR) model. Furthermore, a new observer namely State Space Least Mean Square (SSLMS) observer will be derived. This observer will be used to estimate the states along the propagation path which can not be estimated using LMS algorithm because LMS based on the FIR models. The system is simulated in MATLAB and the results of the pressure modes along the noise path are depicted and have shown that the level of the acoustic signal decreases gradually against the modes. The results of the novel observer to show the comparison of the tracking the pressures of three modes along the interfering region between the primary and secondary path are shown with the mode which is located at the observer achieving accurate estimation.

Key words: Active noise control, state-space model, SSLMS observer, states estimation,

INTRODUCTION

ANC system is a method of reducing unwanted sound. This is realized by artificially generating canceling (secondary) source of sound through detecting the unwanted (primary) noise and processing it by an electronic controller, so that when the secondary wave is superimposed on the primary wave the two destructively interfere and cancellation occurs at the observation point. The schematic diagram of a SISO feedforward ANC structure (Elliot, S.J., 2001; Kuo, S.M. and D.R. Morgan, 1996) is shown in (Fig. 1). Based on the information provided by the reference and error microphones, the weights of ANC controller are adjusted by using of least mean square (LMS) algorithm, and a control signal is generated to drive the secondary loudspeaker (Elliot, S.J., 2001; Kuo, S.M. and D.R. Morgan, 1999). The loudspeaker emits an antinoise signal, which destructs the primary noise around observation point to create a quiet zone around this region.

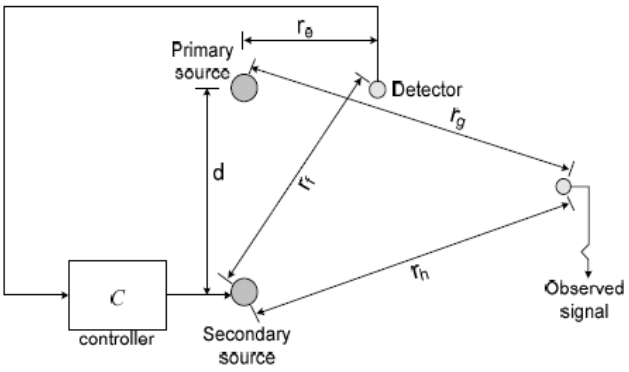

Fig. 1: Schematic diagram of feedforward control structure

Corresponding Author: Mazin T. Muhssin, Department of Electrical & Electronic Engineering, Faculty of Engineering, University Putra Malaysia Selangor Darul Ehsan, Malaysia.
E-mails: {mazinmuhssin, payam_sh26}@yahoo.com, {kamil, hamiruce}@eng.upm.edu.my

The equivalent block diagram of the schematic one is shown in (Fig. 2) where *E, F, G, H* describe state-space characteristics of the acoustic paths through r_e , r_f , r_g , r_h respectively, *C* represents the controller while Y_{DO}, Y_{CO}, and Y_O describe the primary, secondary and combined primary and secondary signals at the observation point, respectively. The feedback path in (Fig. 2) is assumed to be perfectly modeled and cancelled to yield a purely feedforward system (Tokhi, M.O. and R.R. Leitch, 1992)

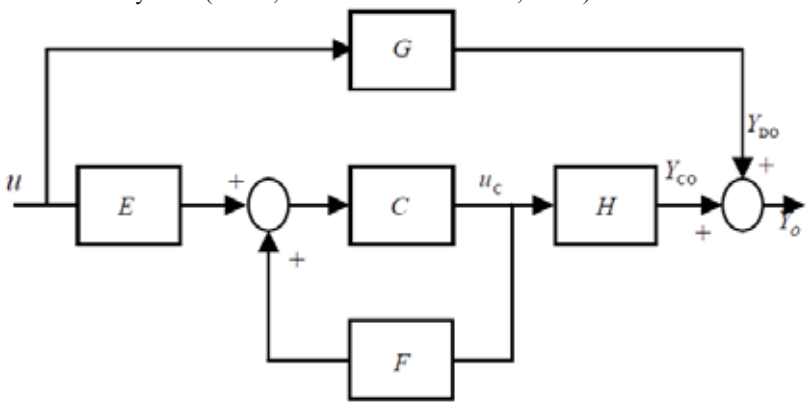

Fig. 2: Block diagram of feedforward control structure

Not many literatures have focused on state-space model of feedforward ANC system. In this paper we will derive a feedforward ANC system by using state-space formulation. A novel algorithm will be constructed to estimate the pressure modes (states) along the interfering which can not be estimated in Finite Impulse Response (FIR) systems. Finally, the simulation results will be presented.

2. Derivation of One Dimensional Propagation Paths:

In order to model a one-dimensional free-field medium, a non reflective wave equation propagating in free-field environment have been assumed, the sound field generated from the loudspeaker and actuator (speaker) in term of pressure are governed from the general form of the wave equation shown in equation (1) (Filippi, P., D. Habault, 1999; Fariba, F. and A.M. Demetriou, 1999).

$$\Delta^2 p(x,t) - \frac{1}{c^2}\frac{\partial^2 p(x,t)}{\partial t^2} = f_c(x,t) \tag{1}$$

where *p(x, t)* is the time dependent acoustic pressure at a point *x* and *c* is the speed of sound in air. The external source is given by

$$f_c(x,t) = u(t)\frac{1}{2ac} Z(X_c - a_c X_c + a_c)(x) \tag{2}$$

where *u(t)* is the input signal, *Z(α, β)(x)* is the boundary condition which is given by

$$Z(\alpha,\beta)(x) = \begin{cases} 1, \ \alpha \le x \le \beta \\ 0 \ elsewhere. \end{cases} \tag{3}$$

Using of Fourier series theory (Filippi, P., D. Habault, 1999; Beranek, L., 1996), the sound wave of finite space problem can be represented by a linear summation of the sinusoidal-wave function [1989] i.e.

$$\psi_n(x,t) = \sum_{n=1}^{\infty} \Psi_v n(t) \Psi_n(x) \tag{4}$$

A method adopted here is to calculate the modes of the traveling wave in the field from known formula (Jesse *et al*, 2006)

$$\Psi_n(x) = \frac{2}{r}\cos(\frac{n\pi x}{r}) \tag{5}$$

Considering a pressure sound wave, the terms $\psi_n\ (x,\ t)$ and $\psi_n\ (t\ )$ can be translated into the sound pressure terms $P_n\ (x,\ t\ )$ and $P_n\ (t\ )$ respectively such that

$$P_n(x,t) = \sum_{n=1}^{\infty} P_n(t)\Psi_n(x) \tag{6}$$

where P_n , ψ_n , r, n, and x are the n^{th} pressure mode and eigen function of the medium, length of medium, no. of modes and arbitrary point respectively.

Applying the orthogonally condition (Al-Bassyiouni, M., B. Balachandran, 2005) and substituting equation (6) and (5) into equation (1) and integrating the resulting equation over the area of the space, the pressure in modal coordinates becomes

$$\ddot{P}_n + \zeta_d w_n \dot{P} + w_n^2 p_n = \rho c^2 \int_A \Psi_n(x) u dA \tag{7}$$

where ζ, w_n , A, ρ are the damping ratio which is introduced to represent the dissipation, the natural frequency of n^{th} ambient pressure mode, the area of the space, and ambient density respectively.
Leting Q equal to the right side hand of equation (7)

$$Q(n) = \int_A \Psi_n(x) u(t) dx \tag{8}$$

The integration over the area of the space can represent the integration from one position to another in the free-field such as the integration from 0 to any arbitrary point x_q.

$$Q(n) = \int_0^{xq} \psi_n(x) u dx \tag{9}$$

Substituting equation (5) into equation (9), yield

$$Q(n) = \frac{2}{r}\int_0^{xq} \cos(\frac{n\pi x}{r}) u(t) dx \tag{10}$$

Solving equation (10), yield

$$Q(n) = \frac{2}{n\pi}(\sin(\frac{n\pi x_q}{r}) - 1)u(t) \tag{11}$$

Where *n1....N,* by leting

$$B(n) = \rho c^2 Q(n) \tag{12}$$

Substituting equation (12) into equation (7), yield the final governing differential equation

$$\ddot{P}_n + \zeta_d w_n \dot{P} + w_n^2 p_n = B(n)u(t) \tag{13}$$

The derivation above can form the state-space model of a feedforward ANC system as described in sections 3.

3. State- Space Model:

The basic principles of state-space models (SSMs) are introduced in (Phillips, L.C. and T.H. Nagle, 1995; Kwakernaak, H. and R. Sivan, 1991). Choosing of SSM over transfer functions has many benefits, such as the numerical reliability, reduce the complexity, minimize the sensitivity, and reduce the computation time (Nijsse, G., M. Verhaegen, 1999). In addition it has the ability to deal with a wide variety of problems including state estimation in control system. In our work the SSM gives the advantages of tracking the modes along propagation path in free-field medium.

In the state space form the relationship between the input and output signals is writen as a system of differential equations using a so called state vector *X*. The above governing equations (5, 6, and 13) can now be used to derive the state-space model. The general state-space form can be writen as

$$\begin{aligned} \frac{d}{dt}X(t) &= AX(t) + Bu(t) \\ y(t) &= CX(t) \end{aligned} \tag{14}$$

where *X* is a state variable, *A* is the dynamics matrix, *B* is the input matrix, *u* is the input vector, y is the output vector, *C* is the output matrix, and *D* is the feedforward matrix which is equal to zero in our work he pressure (states) transform from one point to others in a free-field

$$y_n(x_m, t) = p_n(x_m, t) = CX(t) \tag{15}$$

where $y_n(x_m, t)$ is the pressure output at the observer, and x_m is the location of the observer. In equation (13) we can see that we have two sets of states to represent that each mode has a second order neutrality. Thus

$$x_{2n-1} = P_n \tag{16}$$

$$x_{2n} = \dot{P}_n \tag{17}$$

where *n* is the number of modes *(n =1....N)*. Using of these states along with equations (6), and (13), can form *A , B , C* matrices as depicted in equations (18), and (19) which are considered as the state-space equation of each propagation path with the external source input u in equation (2) and output y in equation (15).

$$X(n+1) = \begin{pmatrix} 0 & 1 & 0 & 0 & & 0 & 0 \\ -w_1^2 & -\zeta w_1 & 0 & 0 & \cdots & 0 & 0 \\ 0 & 0 & 0 & 1 & & 0 & 0 \\ 0 & 0 & -w_1^2 & -\zeta w_1 & & 0 & 0 \\ \vdots & \vdots & \vdots & \vdots & \ddots & \vdots & \vdots \\ 0 & 0 & 0 & 0 & & -w_1^2 & -\zeta w_1 \end{pmatrix} X(n) + \begin{pmatrix} 0 \\ B(1) \\ 0 \\ B(2) \\ \vdots \\ 0 \\ B(N) \end{pmatrix} u(n) \tag{18}$$

$$y(n) = \begin{bmatrix} \psi(1, x_q) & 0 & \psi(2, x_q) & 0 \ldots \psi(N, x_q) & 0 \end{bmatrix} X(n) \tag{19}$$

It has assumed that the propagation signal transfer in one dimensional free field medium in a form of modes. However, the numbers of modes are chosen according to the distance of the propagation paths and separated distance between modes as shown in (Fig. 3). The setup depicted in Fig.3 is assumed for the primary propagation path with length *r = 1000mm* as shown in Fig. 3.7. It is possible to test two modes to calculate the separation distance between them and therefore the total number of modes.

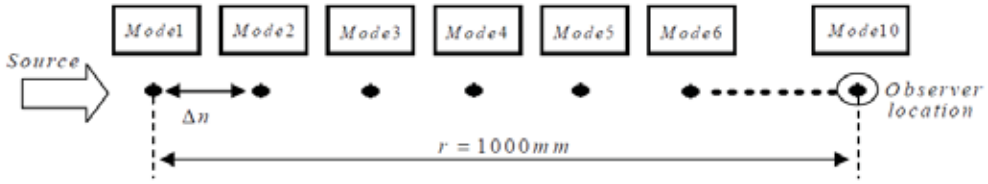

Fig. 3: The pressure (states) transform from one point to others in a free-field

$$NoModes\ (N)= \frac{distance\ of\ the\ propagation\ path\ (r)}{distance\ between\ each\ mode\ (\Delta n)} \tag{20}$$

The number of modes is varying inversely with the distance of each mode while the position of observer is fixed i.e *r* is fixed value.
The first mode is assumed to be calculated at *n* =10*mm* such as

$$\dot{X}[n=100]=\begin{pmatrix}0 & 1\\ -w_1^2 & -\zeta w_1\end{pmatrix}X[n=100] \tag{21}$$

The second path is assumed to be calculated at *n* =3*cm* such that

$$\dot{X}[n=200]=\begin{pmatrix}0 & 1\\ -w_2^2 & -\zeta w_2\end{pmatrix}X[n=200] \tag{22}$$

Thus the separation distance *(Δn)* between each modes is

Δn *(n*= 200*mm*)- *(n*= 100*mm*)= 100*mm*

The relation between the length of path and separation distance between the modes which are distributed along this path can give the total number of modes by applying equation (3.41) such as

$$no.\mathrm{mod}\,es=\frac{r}{\Delta n}=\frac{1000}{100}=10\,\mathrm{mod}\,es \tag{23}$$

However, the same procedure can be used to setup the rest paths and to find the numerical calculation of the derived state space model for the secondary path of ANC system with the parameters value depicted in table 1.

Table 1: Plant Parameters used in Simulation

Parameter	*Values*	*Units*
ρ	1.2	kg/m^3
c	346	*mm/sec*
w	1.08	*rad/sec*
ζ	0.04	_
x_o	300	*mm*

4. Monitoring of Modes Using SSLMS:

An important feature of the system is the ability to monitor the pressure modes along the propagation path. In this paper, a novel state-space observer namely SSLMS observer will be introduced to track the pressure modes at the propagation path. The block diagram of the SSLMS algorithm is depicted in (Fig. 4) where the switch in place of the controller is left open to keep the controller away while the observer is running to perform an offline observation to the states at interfering region. An identification signal *v(n)* is the form of PRBS signal is injected into the secondary propagation path. At the same time the identification signal is also injected into the electronic estimator whose states are adjusted using the SSLMS algorithm to minimize the error signal $e_s(n)$

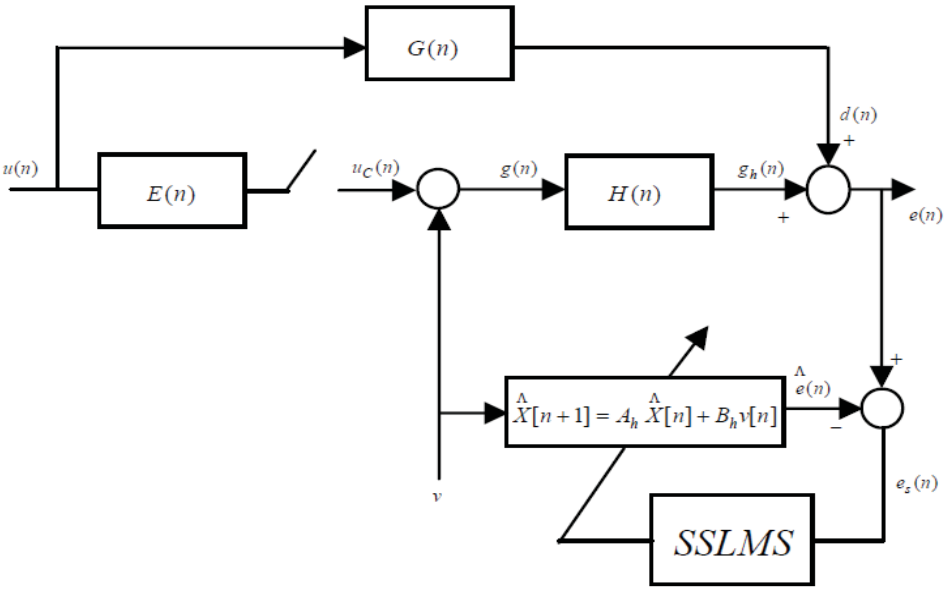

Fig. 4: Block diagram of the SSLMS observer for an ANC system

The derivation and process of the SSLMS algorithm is clarified in (Fig.5) where it uses the prediction and estimation error between the plant error *e[k]* and the output of the estimator $\widehat{e}[k]$which is minimized during the identification process.

The flow of the secondary path estimation can be summarized by the following steps at each iteration

1. We assume that the observation vector *e[n]* start at $n = 1$.
2. Analyze the prediction error ε*[n]*.
3. Compute the prediction state estimate at time *n* using observation up to *n* -1.
4. Define δ*[n]* which is the error between the estimated state $\widehat{X}[k]$ and predicted state $\overline{X}[k]$.
5. Choose $\widehat{X}[k]$ such that the observer error e_s *[n]* equal to zero.
6. Calculate the observer gain *K*.
7. Control the rate of convergence through the step size μ.
8. Return to step 1.

5. Simulation:

In this section, we will simulate the derived model which is presented in section 2 by using MATLAB. The one dimensional geometric arrangement of the feedforward ANC system that is represented by the schematic diagram in (Fig.6) such that the propagation paths have distances r_e =250*mm*, r_f =550*mm*, r_g =1000*mm*, and r_h =200*mm*.

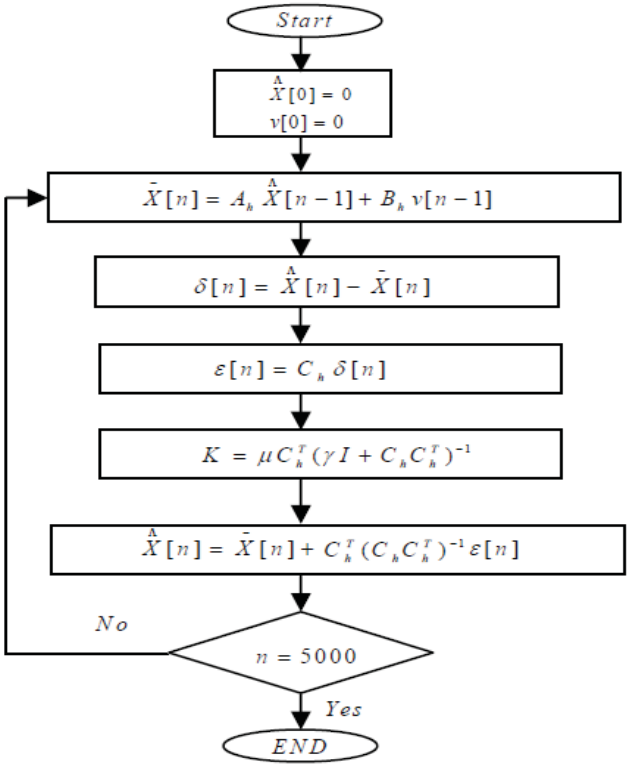

Fig. 5: SSLMS algorithm

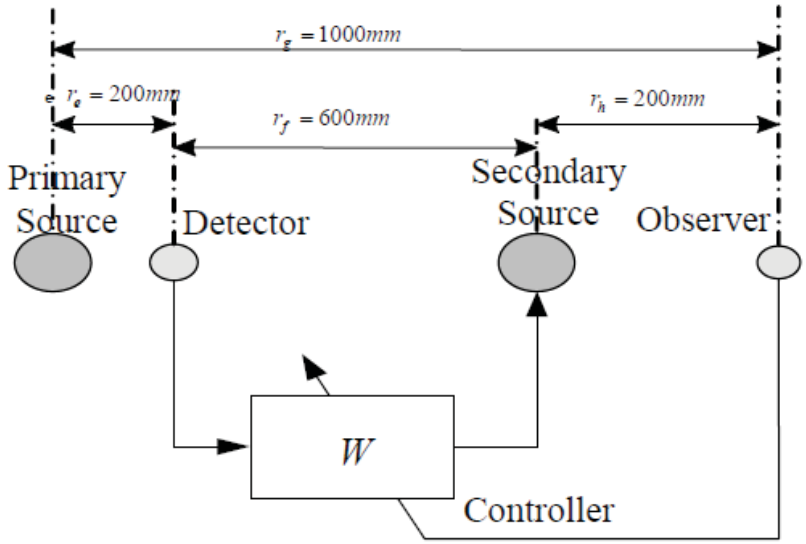

Fig. 6: Schematic diagram of geometrical arrangement within simulation environment

The disturbance signal was set to be random noise with sampling rate 10000 samples throughout the process of modeling. From (Fig. 7) we can find that the level of the acoustic signal decreases gradually against the no. of modes. This indicates that the proposed model is quite good to represent the mechanism of ANC

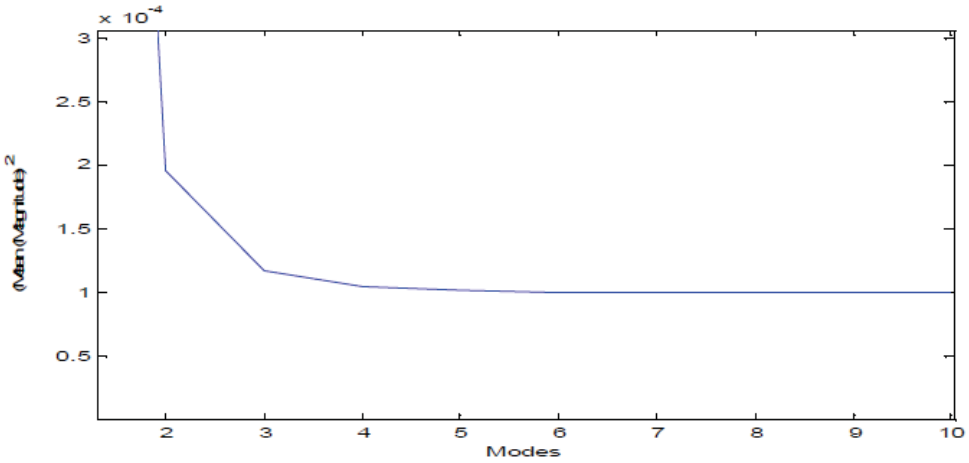

Fig. 7: The Relation between the Average of the Mean Square Amplitude of the Modes against the Number of Modes

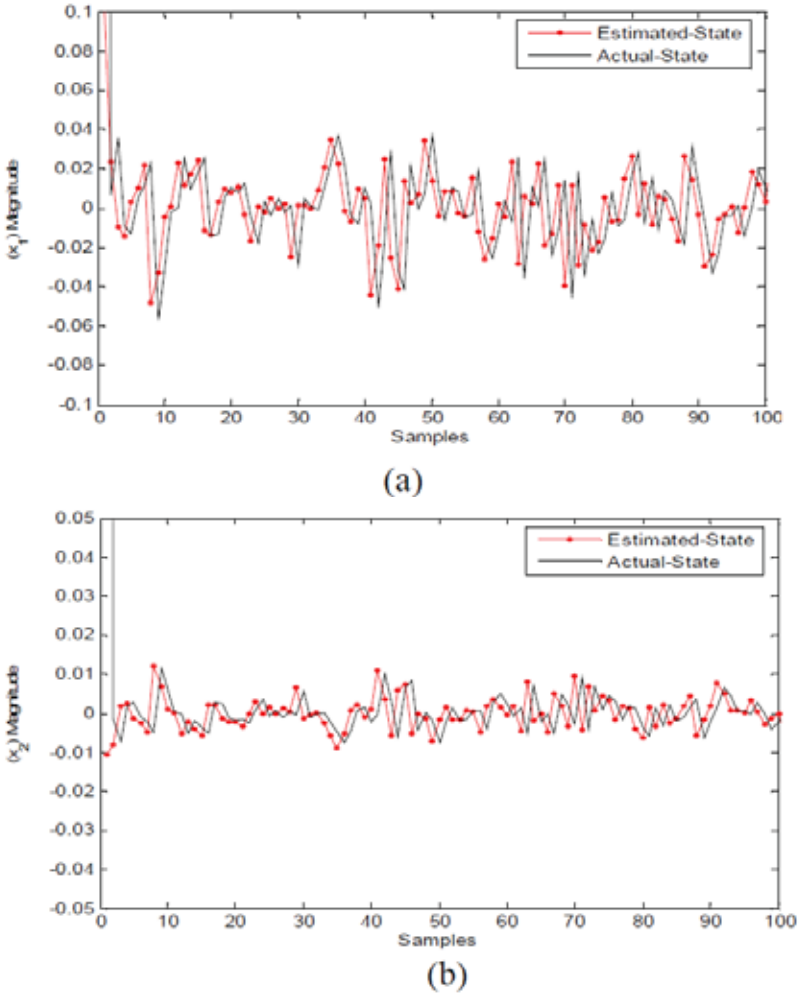

Fig. 8: Comparison of the Secondary Path Real State and Estimated State (a) First State (b) Second State

system because the the level of sound will be desipated as much the mode go a away from the noise source. The length of the secondary path is chosen to be 200*mm* with a separation distance 100*mm* between them such that the simulation is done for two pressure modes along interfering path between the primary path and secondary path. The simulation results of the SSLMS observer are shown in (Fig. 8) where (Fig.8a and b) show the comparison between the secondary path states and the secondary path estimated state by using the SSLMS observer. It can be observed that the secondary path states have been accurately estimated and monitored. The Mean Square Error (MSE) between the actual signal *e(n)* and estimated signal $\hat{e}[k]$ which is referred to the estimator error e_s *(n)* is shown in (Fig.9) and it is found to be 1.5×10^{-3} . The Mean Square Error (MSE) between the actual and estimated signal is shown in (Fig. 9) and is found to be 2.586×10^{-4}.

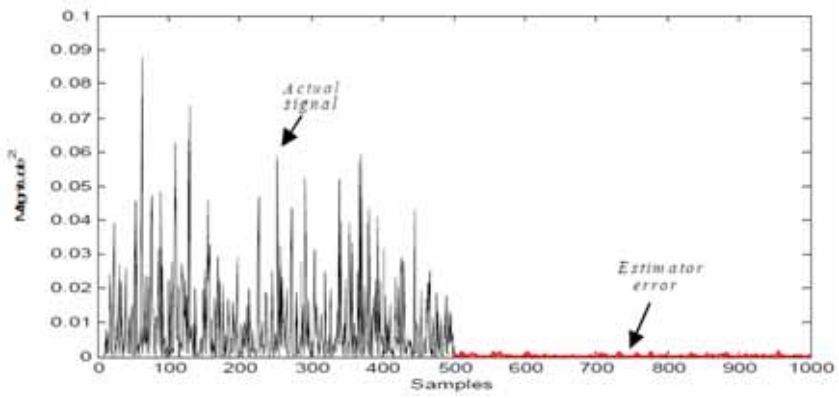

Fig. 9: Comparison between Squared Amplitude of the Actual *e(n)* Signal and Estimator Error $e_s(n)$ Signal

Conclusion:

In this paper, we have developed a model based on state-space formulation to build the proposed mechanism of the ANC system in terms of the length of path, number of modes of each path. The most important contribution in this paper is the development of a novel observer which is namely SSLMS and used to estimate the states (pressure modes) along the propagation path which can not be estimated by using LMS algorithm because such kind of algorithms deals only with FIR systems. The simulation results have approved that the proposed model is quite good to represent the mechanism of ANC system in term of states where the level of the acoustic wave got decrease as the state goes away from the point of the noise source. The comparison of the tracking the pressure at three modes along the interfering region between the primary and secondary path using SSLMS observer have shown an acurate observation.

REFERENCES

Al-Bassyiouni, M., B. Balachandran, 2005. Sound transmission through a flexible panel into an enclosure: structural–acoustics model. Journal of Sound and Vibration, 284(1-2): 467-486.

Beranek, L., 1996. Acoustics. 5th edition McGraw-Hill, United States of America.

Elliot, S.J., 2001. Signal Processing for Active Control. Academic Press, London, UK.

Fariba, F. and A.M. Demetriou, 1999. optimal actuator/sensor location for active noise regulator and tracking control problems. Journal of Computational and Applied Mathematics, 114(1): 137-158.

Filippi, P., D. Habault, J.P. Lefebvre and A. Bergassoli, 1999. Acoustics: Basic Physics, Theory and Methodes. Mathematical composition Seters Ltd, England.

Kuo, S.M. and D.R. Morgan, 1996. Active Noise Control System- Algorithms and DSP Implementations. Wiley, New York, USA.

Kuo, S.M. and D.R. Morgan, 1999. Active noise control: A tutorial review. Proc. IEEE, 87(6): 943-973.

Kwakernaak, H. and R. Sivan, 1991. Modern Signals and Systems. Prentic- Hall Englewood Cliffs, NJ, USA.

Malik, M.B., M. Salman, 2008. State-space least mean square. Signal Process J., 18: 334-345.

Nijsse, G., M. Verhaegen, De. B. Schter, D. Westwick and N. Doelman, 1999. State Space modeling in multichannel active control systems. Proceedings of the 1999 International Symposium on Active Control of Sound and Vibration (Active 99) (S. Douglas, ed), Fort Lauderdale, Florida, pp: 909-920.

Phillips, L.C. and T.H. Nagle, 1995. Digital Control System Analysis and Design. 3rd edition, Prentice Hall, Inc., United Kingdom.

Tokhi, M.O. and R.R. Leitch, 1992. Active Noise Control. Oxford:Clarendon Press.